

EFFICIENCY POTENTIAL OF SOLAR CELLS BASED ON COMPENSATED MULTICRYSTALLINE SILICON MATERIALS

D.S. Saynova¹, G. Coletti¹, M. Di Sabatino^{2*} and L.J. Geerligts¹

¹ECN Solar Energy, PO Box 1, 1755 ZG Petten, the Netherlands

Tel: +31-224-564093; Fax: +31-224-568214; E-mail: saynova@ecn.nl

²SINTEF Materials and Chemistry, A. Getz v. 2B, 7465 Trondheim, Norway

* present address: NTNU – Department of Materials Science and Engineering, NO-7491 Trondheim, Norway

ABSTRACT: The purpose of the present work is evaluation of the impact of Cr-contamination on solar cell properties of compensated multicrystalline silicon (mc-Si) ingots. Cr is an effective recombination centre of practical relevance. Studying its effects in compensated material allows monitoring the dependence of solar cell characteristics on resistivity. Therefore, two compensated materials were investigated: with and without addition of 20 ppm wt Cr to the high-purity Si feedstock. Lifetime measurements on as-cut wafers showed more than one order of magnitude decrease in case of Cr-containing samples. Solar cell manufacturing was accomplished for p-type wafers utilizing two different emitter sheet resistances and a conventional industrial screen-print process. It was found that gettering and hydrogenation involved in cell processing significantly improved material properties in the presence of Cr. As a result cell performance was comparable to the compensated reference. Efficiencies of p-type cells in the range of 15.7% were achieved for this heavily Cr-contaminated, compensated mc-silicon of a resistivity of 4 Ohm.cm.

Keywords: multicrystalline silicon, impurities, solar cells, compensation

1 INTRODUCTION

During the last years a significant development has been carried out on low-cost feedstock (e.g. upgraded metallurgical grade, UMG) as an alternative to electronic grade (EG) silicon, which is purified using an energy-consuming complex procedure. UMG material typically contains elevated levels of transition metal impurities (such as Cr) that may adversely affect solar cell performance [1-6]. Another characteristic of UMG feedstock is presence of dopants like B and P resulting in a compensation effect which can also be used to obtain resistivity values in a range suitable for solar cell-applications [7-11]. There have been reports of reduced bulk lifetime in presence of compensation [7, 10], and a reduced majority carrier mobility according to the Klaassen's model, as well as a somewhat more reduced minority carrier mobility [12]. In addition, dependent upon solar cell design, high base resistivity, which occurs in part of the ingot due to compensation, can cause efficiency loss [11], but can also reduce the recombination activity of impurities. Therefore, a study of the impact of metal impurities on solar cell performance of compensated materials is highly relevant.

A particular benefit of studying impurity effects in compensated ingots, is that part of such ingots shows a rapid variation in resistivity versus position (i.e., from wafer to wafer). This allows for investigation of the effect of resistivity on impact of impurities, with minimal disturbance from other changes such as changes of crystal defect structure.

This paper presents a study of the impact of Cr-contamination in combination with compensation on solar cell properties of multicrystalline silicon (mc-Si) ingots. Feedstock was based on high purity silicon that was intentionally doped with both P and B, and with and without addition of Cr. Material transition from p-type to n-type along the ingot allowed for a comprehensive study of the effect of Cr in compensated mc-Si silicon. The solar cells were processed using conventional industrial conditions. Two emitters of different sheet resistance (R_{sheet}) were utilized, effectively varying the gettering. Testing the effect of Cr in n-type silicon at cell level

would be interesting but has not yet been done.

2 EXPERIMENTAL DETAILS

2.1 Materials

Two multicrystalline (mc) silicon ingots were grown in Crystalox DS250 directional solidification furnace at SINTEF using EG polysilicon with B and P dopants added to the feedstock before crystallization. The additions were 0.14ppm wt and 0.74ppm wt for B and P, respectively. This resulted in two compensated materials (labeled REF and Cr), in which p-type to n-type transition region occurred at about 70% block height. One of the ingots (Cr) also had an addition of 20ppm wt Cr to the feedstock before crystallization.

Resistivity distribution along the two ingots (Figure 1) was measured by four point probe (FPP). The reference and Cr-contaminated ingots had the same addition of B and P to the EG feedstock (i.e. same compensation level). A transition from p-type to n-type was observed at approximately 70% ingot height in both castings as shown in Figure 1, due to different segregation coefficient of B ($k=0.8$) and P ($k=0.35$). The marked ranges in the plots refer to wafers available for further investigations after wafer cutting (due to accidental breakage during wafering, wafers outside the marked ranges were not available).

As illustrated by Figure 1(a) only a limited amount of reference p-type wafers were available, the bulk resistivity of which was far beyond the typical range for solar cell applications. (>220hm.cm).

2.2 Lifetime samples in as-cut state

Bulk minority carrier lifetime in as-cut state was measured at one position in the middle of the wafers using QSSPC technique. The samples were polished by removing 20 — 25µm of the total thickness and cleaned thoroughly before coating with surface-passivating SiNx. Further, µW-PCD was used to obtain spatially resolved lifetime mapping.

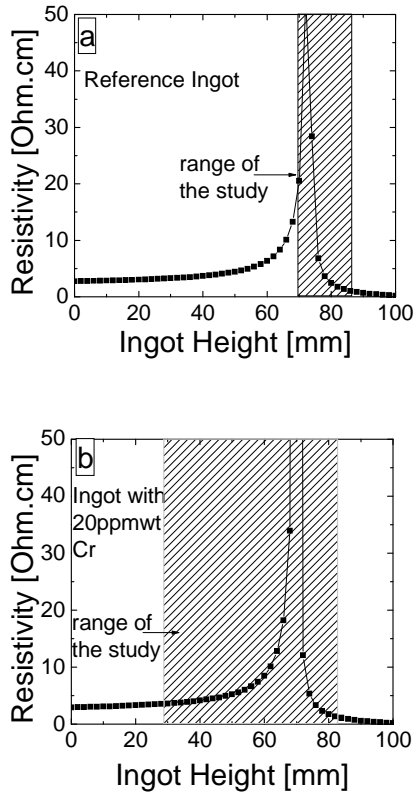


Figure 1: Resistivity profile for the reference (REF) – (a) and Cr-containing ingot (b). The marked areas in each plot denote the material remaining after the wafering stage.

2.3 Solar cell preparation and measurements

p-type solar cells with an area of $125 \times 125 \text{ mm}^2$ were prepared from the reference (p-REF) and the material with Cr content (p-Cr), employing standard ECN p-type cell processing conditions [13] and using two different emitters of high and low sheet resistance (R_{sheet}).

The I-V characteristics of the solar cells under illumination were measured with a sun simulator under 1sun STP.

3 RESULTS AND DISCUSSION

3.1 Materials

3.1.1. Effect of Cr-contamination

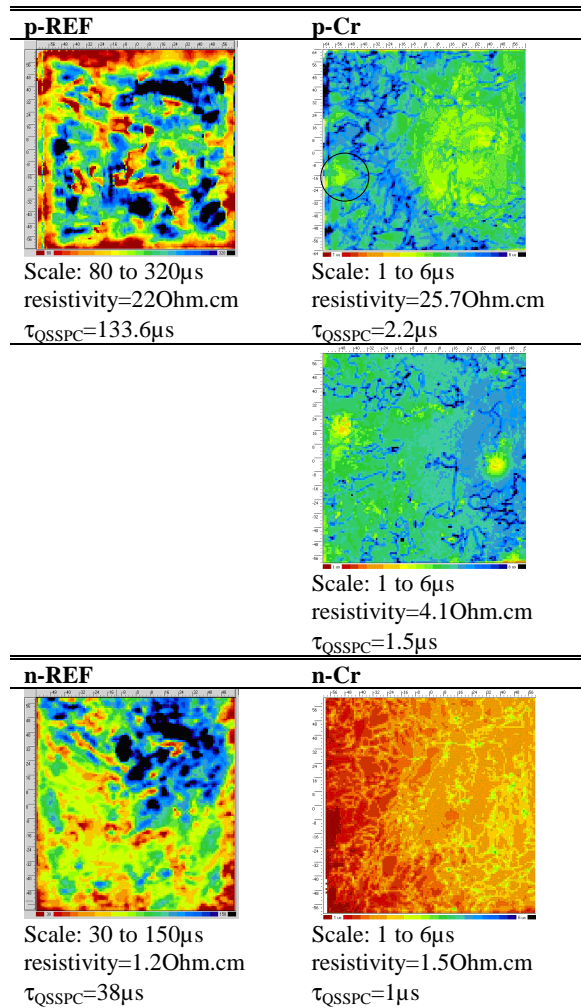
The impact of Cr-contamination on material properties was evaluated using lifetime measurements on as-cut wafers of a comparable resistivity from p-type and n-type parts of the reference and Cr-containing ingots. A summary of QSSPC-lifetime values measured at a minority carrier density of $1 \times 10^{15} \text{ cm}^{-3}$ and $\mu\text{W-PCD}$ -maps is shown in Table I. The results demonstrated drastic lifetime decrease for Cr-contaminated ingot compared to the reference for both p-type and n-type materials. Note that the lifetimes for the p-type and n-type wafers in this Table are not directly comparable because they have very different resistivity.

3.1.2 Influence of compensation

The compensation effect was studied for p-Cr

material using lifetime measurements and resistivity mapping. Lifetime of p-Cr, measured by QSSPC in the available resistivity range, was markedly low: between 1.8 and $2.2 \mu\text{s}$ with no apparent variation with the ingot position. In addition, for higher resistivity, e.g. $>13.8 \text{ Ohm.cm}$, that was also closer to the p-n transition point, some low lifetime areas (Table I, marked with a circle) were related to local changes in the base resistivity within the wafer. The latter effect was caused by the non-flat solidification profile which in combination with the different segregation coefficients of B and P resulted in an inhomogeneous resistivity over the surface of wafers near the p-n transition of the ingot.

Table I: Examples for QSSPC-values and lifetime maps measured on as-cut wafers from the compensated reference (REF) and Cr-contaminated ingots at comparable resistivity values. The circle-mark on the high resistivity p-Cr sample denotes low lifetime location also found as high recombination area in the solar cells by using IR lock-in-thermography technique and to be discussed in section 3.2.



3.2 Solar cell performance

The results described in this section refer to a cell area of $98 \times 98 \text{ mm}^2$. By cutting off the edges of the cells, severe shunting that appeared especially for higher base resistivity ($>13.8 \text{ Ohm.cm}$) was avoided. IR lock-in-

thermography images of those cells revealed locations of high recombination that corresponded to areas of material type change, as discussed in 3.1.2

3.2.1. Cr-contamination

A comparison with the reference ingot to evaluate the effect of Cr contamination was possible for a limited amount of data at significantly high base resistivity. This was due to the fact that p-REF was available only for the base resistivity of 22.5 Ohm.cm, albeit including emitter variation (Figure 2). In that resistivity range the solar cell performance demonstrated no detrimental effect of the Cr presence. This was an indication that both processing schemes in our study achieved a good and effective Cr gettering, avoiding impaired solar cell parameters.

3.2.2. Base resistivity effect for solar cell processing using two emitter types

The effect of base resistivity on the p-type cell parameters for two emitter processing schemes was evaluated only for p-Cr (Figure 2), because the range of p-REF was insufficient for this purpose (see Figure 1(a) and the comments in section 2.1).

For both processing groups of p-Cr (Figure 2(a)) J_{sc} increased until 15 Ohm.cm after which it stabilized. As the lower resistivity range was also closer to the crucible walls, presence of impurities in higher concentrations can be expected causing recombination and thereby decreasing J_{sc} . Also it is known that Shockley-Read-Hall (SRH) recombination generally increases with lower resistivity. Higher emitter R_{sheet} resulted in J_{sc} increase, probably as a result of reduced emitter and/or surface recombination, and/or effectiveness of gettering.

Interestingly, for p-Cr the V_{oc} -trend towards base resistivity strongly depended on cell processing. In particular, for the low-ohmic emitter V_{oc} displayed little sensitivity on base resistivity (open symbols in Figure 2(b)). For the high emitter R_{sheet} -group of p-Cr there was a continuous and significant V_{oc} -decrease from 608mV to 590mV as the resistivity reached 22.4 Ohm.cm (closed symbols in Figure 2(b)). In this way V_{oc} behavior of p-Cr for the high-ohmic emitter was mainly influenced by the net doping.

Increase in base resistivity had reverse effect on FF for both emitters (Figure 2(c)). However, there was a stronger impact on high R_{sheet} emitter, with FF decrease of (2.8+0.3)% absolute in high base resistivity range. In case of low R_{sheet} the decrease in FF was less pronounced amounting to (1.5+0.2)% absolute. Low R_{sheet} emitter yielded higher FF values.

The cell efficiency at low base resistivity was (15.7+0.2)% and comparable for both emitters (Figure 2(d)). This was probably due to the similar V_{oc} and slightly higher FF, which compensated for the lower J_{sc} values for low R_{sheet} . Further, at elevated base resistivity values cells with high R_{sheet} -emitter had efficiency significantly reduced to 14.9%. Similar strong trend with base resistivity was observed for V_{oc} and FF of this emitter as discussed above. For the low R_{sheet} group efficiency remained stable with base resistivity which was consistent with the V_{oc} characteristic.

The obtained upper efficiency limit was about 0.4 % absolute lower than typical solar cell performance achievable with the applied processing conditions on standard, non-compensated mc-Si wafers of a similar size and resistivity (1±0.2) Ohm.cm. Nevertheless, this is a

remarkably good result, since the lifetime values of p-Cr material at the beginning of the processing are significantly lower than the reference (Table I), and at least a factor of 10 below typical bulk lifetime of standard mc-Si wafers. These results support earlier studies on effective increase in bulk lifetime up to two orders of magnitude of Cr-contaminated materials using a combination of gettering phenomena and hydrogenation [14-15].

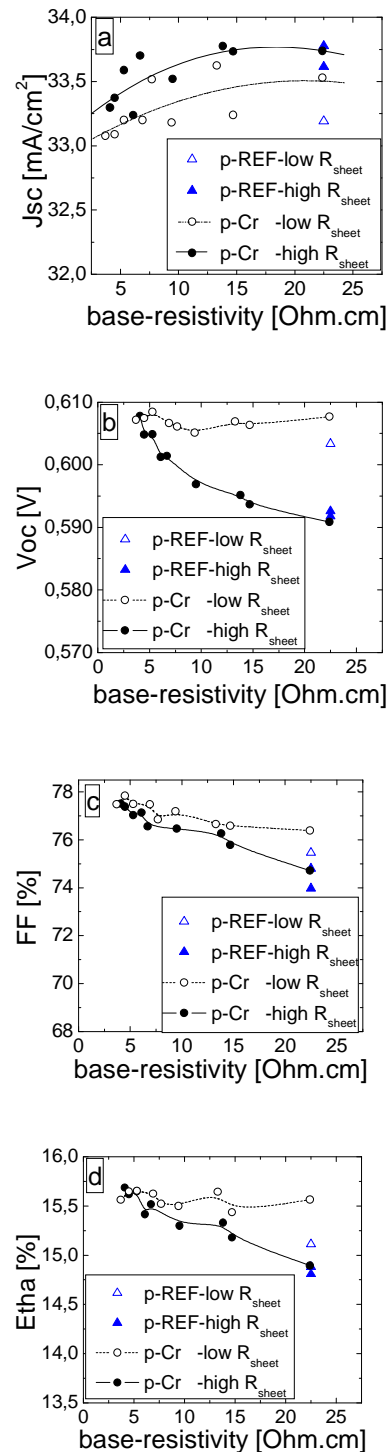


Figure 2: Solar cell characteristics versus wafer base resistivity for the reference (p-REF) and Cr-doped material (p-Cr).

3.2.3. Analysis of spectral response

The dependence of spectral response upon base resistivity and emitter processing of the solar cells was also investigated. For this purpose, for each emitter type three groups of solar cells from the p-Cr ingot were selected with respect to the bulk resistivity. The low resistivity group was of 4.5 Ohm.cm. The medium values were between 6 and 7 Ohm.cm, respectively. Finally, the highest bulk resistivity selected for the IQE measurements was between 13 and 15 Ohm.cm.

At first, the base resistivity effect on the IQE was evaluated for each emitter separately (Figure 3(a) for low R_{sheet} -emitter). Therefore, relative IQE was calculated as a ratio between low base resistivity data and each of the two higher resistivity sets of samples. It should be noted that a similar trend was found for the high R_{sheet} -emitter as well. The strongest effect of base resistivity on IQE was in the long wavelength region. At 1 μ m wavelength, characteristic for bulk diffusion length, IQE increased with base resistivity. This result can be due to an enhanced SRH lifetime at lower net-doping density. A summary of the minority carrier diffusion length (L_{diff}) calculated from Basore-fit ($1/IQE$ vs. $1/\alpha(\lambda)$) of the long wavelength part of IQE spectrum is shown in Table II for both emitters at varied bulk resistivity. For both processing schemes L_{diff} increased with resistivity.

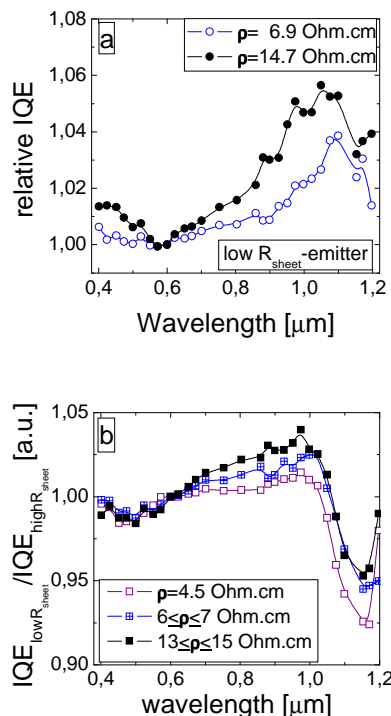


Figure 3: Relative IQE characteristics: (a) effect of base resistivity in case of low-ohmic emitter cells and (b) impact of emitter processing for three ranges of base resistivity (ρ).

Table II: Minority carrier diffusion length (L_{diff}) calculated from Basore-fit of the long wavelength IQE characteristics for each emitter type and varied resistivity

Emitter R_{sheet}	Resistivity [Ohm.cm]	L_{diff} [μ m]
low	4.5	633
	6.9	692
	14.7	760
high	4.5	610
	6.1	643
	13.8	723

Further, impact of cell processing on IQE was studied using as ratio between low- and high-ohmic emitter groups calculated for each bulk resistivity range (Figure 3(b)). There was a slight increase in the short wavelength range for the high-ohmic emitter, indicating reduced emitter and/or surface recombination also supported by the larger J_{sc} as described in the I-V results. In the long wavelength range, performance of low-ohmic emitter was better as expected due to the increased diffusion length values outlined in Table II. These results revealed an improved gettering and hydrogenation effects in case of low-ohmic emitter consistent with higher V_{oc} values (Figure 2(b)). At a wavelength of 1.1 μ m, cell performance for the high-ohmic emitter improved, possibly due to reduced free carrier absorption at lower doping levels.

4 SUMMARY AND CONCLUSIONS

The main result of this investigation is that presence of Cr in 20ppm wt does not impair solar cell performance of compensated p-type mc-Si grown by a dedicated process in directional solidification furnace. Although lifetime in as-cut state was drastically reduced due to Cr-contamination, the p-type material quality was significantly improved by using industrial-type cell processing steps which involved gettering and hydrogenation. Consequently a very good cell performance was demonstrated with efficiency reaching 15.7% at p-type wafer resistivity of about 4 Ohm.cm. The experiments indicated that even higher performance can be realized for wafer resistivity values within the common application range between 1 and 2 Ohm.cm.

With respect to the compensation effect, results for p-type Cr-containing material demonstrated that bulk resistivity impact on solar cell parameters can be tuned through emitter processing.

5 ACKNOWLEDGEMENTS

This work was financed by the European projects "CrystalClear Integrated Project" (SES6-CT_2003-502583) and "Foxy-Development of solar grade silicon feedstock for crystalline wafers and cells by purification and crystallization" (SES6-019811), and subsidized by the Dutch Ministry of Economic Affairs.

6 REFERENCES

- [1] D. Macdonald, L.J. Geerligs, *Applied Physics Letters*, 85, (2004) 4061.
- [2] L.J. Geerligs, P. Manshanden, I. Solheim, E.J. Øvrelid, A.N. Waernes., *Proceedings 21st European Photovoltaic Solar Energy Conference (2006)* 1285.
- [3] G. Coletti, P.C.P. Bronsveld, C. Knopf, C.C. Swanson, R. Kvande, L. Arnberg, H. Habenicht, W. Warta., *Proceedings 24th European Photovoltaic Solar Energy Conference (2009)* 1011.
- [4] G. Coletti, P. Bronsveld, G. Hahn, W. Warta, D. Macdonald, B. Ceccaroli, K. Wambach, N. Le Quang and J.M. Fernandez. Accepted for publication in *Advanced Functional Materials* 2010. DOI: 10.1002/adfm.201000849
- [5] M. Hystad, C. Modanese, M. Di Sabatino, L. Arnberg, A-K. Sjøiland, A. Holt, *3rd International Workshop on Crystalline Silicon Solar Cells (2009)*.
- [6] S. Binetti, J. Libal, M. Acciarri, M. Di Sabatino, H. Nordmark, E.J. Øvrelid, J.C. Walmsley, R. Holmestad, *Mat. Sci. and Eng. B* 159-160 (2009) 274.
- [7] J. Libal, M. Acciarri, S. Binetti R. Kopecek, R. Petres, C. Knopf, K. Wambach, *Proceedings of the 22nd European Photovoltaic Solar Energy Conference (2007)* 1124.
- [8] E. Good, R. Kopecek, J. Arumughan., *Proceedings of the 23rd European Photovoltaic Solar Energy Conference (2008)* 1218.
- [9] B. Herzog, G. Hahn, C. Knopf, K. Wambach., *Proceedings 24th European Photovoltaic Solar Energy Conference (2009)* 1015.
- [10] D. Macdonald, A. Cuevas, M. Di Sabatino, L.J. Geerligs., *Proceedings of the 23rd European Photovoltaic Solar Energy Conference (2008)* 951.
- [11] J. Libal, S. Novaglia, M. Acciarri, S. Binetti, R. Petres, J. Arumughan, R. Kopecek, and A. Prokopenko, *J. Appl. Phys.* 104 (2009) 104507.
- [12] F. Rougieux et al., *J. Appl. Phys.* **108**, 013706 (2010).
- [13] P.C.P. Bronsveld, R.C.G. Naber, L.G. Geerligs, S. Pozigun, M. Syversten, C. Knopf, R. Kvande, *Proceedings 24th European Photovoltaic Solar Energy Conference (2009)* 1137.
- [14] P. Manshanden, G. Coletti, L.J. Geerligs, A.C. Veltkamp, *3rd International Workshop on Crystalline Silicon Solar Cells (2009)*.
- [15] M. Blazek, W. Kwapil, J. Schön, W. Warta., *Proceedings 24th European Photovoltaic Solar Energy Conference (2009)* 1015.